April 7 2017

Correlative Light and Electron Microscopy on Mouse Polyomavirus-Infected Fibroblasts

By: Christina Henderson
The Garcea Laboratory

Defense Committee:

Dr. Robert Garcea, Thesis Advisor

Dr. Jennifer Martin, Honors Council Representative

Dr. Michaele Ferguson, Out of Department Member

1. Abstract

Polyomaviruses are small, DNA tumor viruses that can infect multiple species, including humans. In recent years, the number of identified human polyomaviruses (huPyV) has grown. To identify possible therapeutic targets for huPyVs, a better understanding of virus infection at the structural level is needed. Confocal microscopy allows for the visualization of fluorescently-tagged proteins but without seeing the cell's subcellular structures, functional information can be lost. Electron microscopy provides structural insight but does not always provide biological or biochemical details. Combining these two approaches can relate biological function to structural information about virus replication. Polyomaviruses (PyV) co-opt host proteins that function during normal DNA damage repair to aid in replication of viral genomes. Here we describe a mouse embryonic cell line (MEF) that stably expresses a fluorescently-tagged component of the replication protein complex A (RPA). RPA is made up of three proteins (RPA70/RPA32/RPA14) and is an important host component for PyV vDNA replication. MEFs stably-expressing GFP-human RPA32 or RPA70 (GFP-huRPA32/70) were infected with murine polyomavirus (MuPyV) to study viral DNA (vDNA) replication by correlative light and electron microscopy (CLEM). Light microscopy studies found that GFP-huRPA32/70 localized to sites of vDNA replication along with other host DNA damage response (DDR) proteins, which have been previously characterized. We attempted to correlate the immunofluorescence of GFP-huRPA proteins at viral replication centers to the ultrastructure of virus factories that have been observed by electron microscopy (EM).

2. Introduction

Polyomaviruses (PyVs) infect different types of mammals and birds (reviewed in Decaprio & Garcea, 2013). Until recently, two human polyomaviruses (HuPyVs) have been studied: JC polyomavirus (JCPyV) and BK polyomavirus (BKPyV) (Gardner, et al., 1971). Serological studies indicate that BKPyV infects up to 90% of the general population and JC infects greater than 50% of the general population (Hirsch et al., 2003; Rinaldo et al., 2013). BKPyV and JCPyV infection typically occurs during childhood and results in a lifelong infection that is asymptomatic for healthy individuals (Maginnis et al., 2014; Rinaldo et al., 2013). Severe pathological manifestations appear in patients who are immunocompromised (Hirsch et al., 2003). The tumorigenic effects of PyV infection have been studied for over twenty years in murine polyomavirus (MuPyV) and have provided crucial insight regarding the cellular and molecular biology of PyVs (Cheng et al., 2009; Guy et al., 1992; Decaprio & Garcea, 2013).

PyVs are non-enveloped, dsDNA tumor viruses that replicate in the host cell's nucleus. The 5-kb circular, DNA genome can be divided into two regions, early and late, which encode up to six genes, depending on the strain. The early region encodes the T antigens, which are responsible for priming the cell for vDNA replication (Myers et al., 1981). MuPyV encodes three T antigen proteins, small, middle, and large T antigen (ST, MT, LT), which arise from splicing variations during transcription. The late region encodes the viral capsid proteins (VP1, VP2, and VP3) (Yan et al., 1996; Klein, 1980). VP1 is the major viral capsid protein, whereas VP2 and VP3 are the smaller, minor capsid proteins (Yan et al., 1996; Klein, 1980). MuPyV is a 45 nm icosahedral viral capsid (Yan et al., 1996; Klein,

1980). The viral capsid is composed of 72 capsomeres, formed from one molecule of VP2 or VP3 associated to a VP1 pentamer (Fig 1) (Barouch & Harrison, 1994).

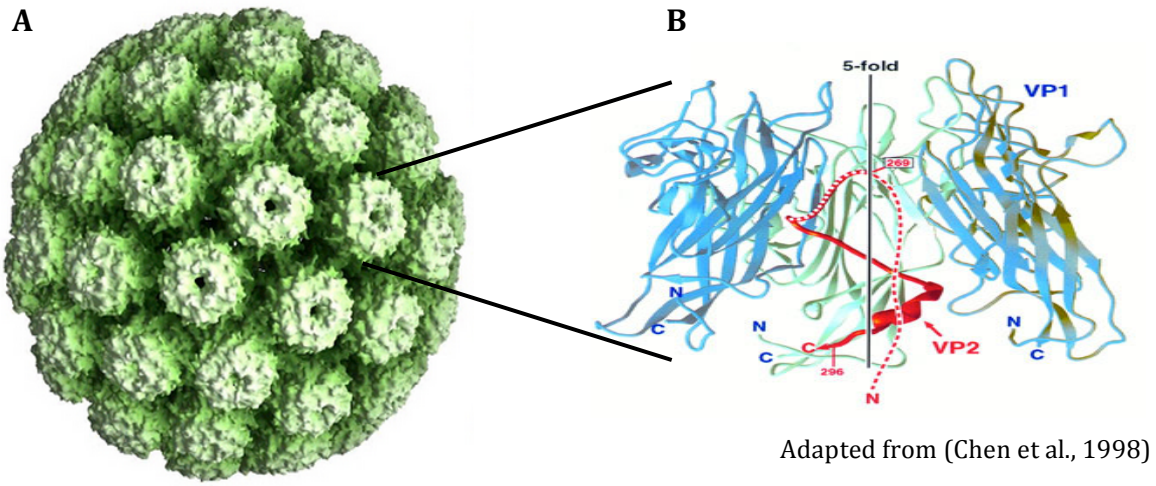

Adapted from (Chen et al., 1998)

Figure 1. (A) Cryo-EM of the MuPyV capsid composed of 72 capsomeres (VP1 pentamers associated to a molecule of VP2 or VP3). (B) A structural model of an SV40 VP1-VP2 complex

PyVs infect cells by binding sialic acids residues on the host's cell surface via VP1 (Tsai et al., 2003). PyV is internalized and trafficked to the endoplasmic reticulum in a microtubule-dependent manner (Norkin et al., 2002; Gilbert et al., 2003). In order for the virus to traffic to the cytosol and eventually the nucleus, it co-opts endoplasmic reticulum-associated degradation (ERAD) translocation complex proteins (Goodwin et al., 2011; Bennett et al., 2013). The virus gains entry into the nucleus using a nuclear localization signal on a viral capsid protein (Neu et al., 2009; Nakanishi et al., 2007). Once in the nucleus, the early genes are expressed, and LT drives the cell into S phase. Studies using simian virus 40 (SV40) have demonstrated LT's ability to sequester the tumor suppressor, p53, and compromise checkpoint control of G1 to S phase (Damania et al., 2009). In addition, LT binds the retinoblastoma tumor suppressor (Rb) protein family, leading to the

activation of downstream genes essential for entry into S phase (Damania et al., 2009). Once the cell has entered into S phase, MuPyV uses the cell's machinery to promote viral DNA (vDNA) replication. After LT unwinds double-stranded DNA (dsDNA) using its helicase domain, it recruits the host's polymerase/primase complex to the viral origin of replication and initiates synthesis (Damania et al., 2009). Following DNA replication, the viral capsid proteins are expressed (Kawano et al., 2006). The viral capsid proteins form capsomeres in the cytosol, are transported into the nucleus, and by unknown mechanisms, package vDNA (Kawano et al., 2006). The virus spreads by lysing the host cell, thereby releasing the virions (Damania et al., 2009).

In addition to using the host's replication machinery, LT uses the host's DNA damage response proteins (DDR) to promote vDNA replication. One of the earliest complexes recruited to sites of DNA damage is the MRN complex (D'amours et al., 2002). The MRN complex is a trimeric complex made up of three proteins, Mre11, Rad50, and Nbs1 (D'amours et al., 2002). The MRN complex binds double-stranded DNA (dsDNA) breaks and recruits ataxia-telangiectasia mutated (ATM) kinase to sites of DNA damage (Zhao et al., 2008). The MRN complex is phosphorylated by ATM then activates ATM to phosphorylate downstream substrate proteins (Zhao et al., 2008). Phosphorylated ATM (pATM) kinase initiates a signaling cascade that triggers p53-mediated G1 to S phase checkpoint arrest to promote DNA repair (Kastan et al., 2004; Shiloh 2003). During SV40 infection, the MRN complex may act in viral replication centers to maintain ATM activation (Zhao et al., 2008). Inhibition of ATM during SV40 replication results in a loss of viral replication centers, indicating that the activation of ATM, maintained by MRN, may be necessary for the infected cell to remain in S phase (Zhao et al., 2008).

The DDR protein, γH2AX, is important for maintaining repair enzymes around DNA break sites while preventing progression of the cell cycle (Bassing et al., 2002; Celeste et al., 2003; Matsuoka et al., 2007). Upon infection, H2AX is phosphorylated at serine 139 by pATM (Kastan et al., 2004). Although γH2AX is not essential for MuPyV genome replication and virus assembly, it plays an important role in recruiting DDR proteins and promoting their activation (Heiser et al., 2016).

A DDR protein required for the replication of chromosomal DNA and SV40 replication is replication protein A (RPA) (Kenny et al., 1990). RPA is a heterotrimeric single-stranded DNA (ssDNA) binding protein essential for DNA replication and repair pathways such as homologous recombination (Fanning, 2006). The RPA heterotrimer is comprised of a 70-kD subunit (RPA70), a 32-kD subunit (RPA32), and a 14-kD subunit (RPA14) (Han et al., 1999). The complex has four ssDNA binding sites, one within RPA32 and three within RPA 70 (Fanning, 2006). RPA32 is phosphorylated at serine 23 (RPA32-pSer23) in a cell-cycle dependent manner and in response to DNA damage (Fotedar & Roberts, 1992). Although it is unclear if RPA32-pSer23 is required for MuPyV replication, activation of RPA32 upon DNA damage allows for the recruitment of additional DDR proteins (Hendricksen et al., 1996; Justice et al., 2015). It has been shown that LT's origin binding domain (OBD) associates with RPA32 and RPA70 and weakens RPA's binding to ssDNA (Fig 2) (Fanning, 2006). RPA's lowered affinity for ssDNA results in a strand of DNA being released; LT uses the cell's machinery to replicate the viral genome (Fanning, 2006).

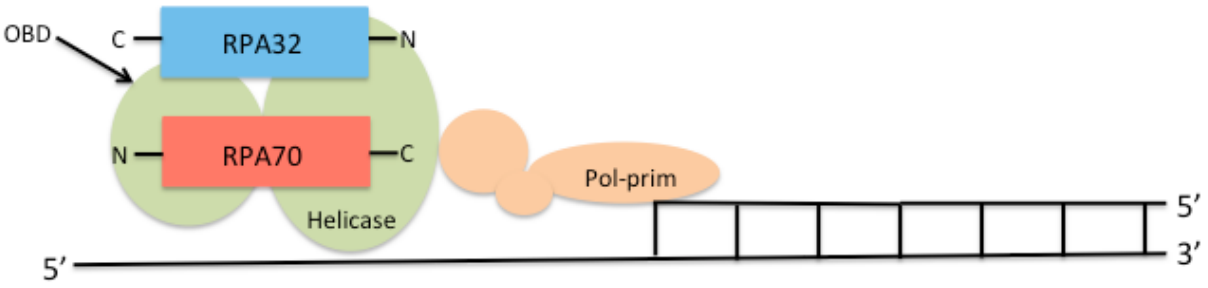

Adapted from (Arunkumar et al., 2005; Fanning et al., 2006)

Figure 2. SV40's LT associates with RPA32 and RPA70 subunits and utilizes the host's machinery to replicate its genome: green shapes depict LT's helicase and origin-binding domains (OBD); orange shapes depict the host's polymerase-primase binding to the DNA.

In addition, MuPyV utilizes ataxia-telangiectasia and Rad-3 related (ATR) kinase, a DDR protein, to replicate its genome (Ciccia et al., 2010). ATR is recruited by RPA upon DNA damage and can target the checkpoint protein, Chk1 (Ciccia et al., 2010). In turn, Chk1 phosphorylates chromatin-bound proteins to promote stability of the replication fork (Ciccia et al., 2010). During infection, activated Chk1 (pChk1), may play a role in S phase cell cycle arrest (Justice et al., 2015; Liu et al., 2000). pChk1's role in MuPyV is still be investigated as recent data has shown that Chk1 is not required for MuPyV replication or assembly (Heiser et al., 2016).

It has been shown previously that MuPyV activates and reorganizes host DDR proteins in the nucleus. Activated RPA32 localizes to vDNA replication centers along with DDR signaling proteins pATM, pChk1, and γH2AX (Heiser et al., 2016). By electron microscopy, we observed tubular structures adjacent to progeny virions in infected murine embryonic fibroblasts (MEFs). The tubular structures are composed of the capsid protein, VP1, and are thought to be an assembly intermediate during encapsidation of the viral genome. These tubular structures, together with progeny virions, are called "virus factories" (Erickson et al., 2012). It is unknown how vDNA replication centers and DDR

protein localization observed by immunofluorescence analysis (IFA) correlate to virus factories observed by EM.

Correlative light and electron microscopy (CLEM) is an imaging technique that complements the capabilities of the electron microscope (EM) and the light microscope (LM) (Perkovic et al., 2014). CLEM combines the ability of LM to view fluorescently tagged proteins with EM's ability to provide high-resolution images of the morphology and ultrastructure of the location where the protein resides (Perkovic et al., 2014; Hodgson et al., 2014). CLEM has three essential phases after LM imaging: find a suitable probe, process the sample, and analyze the cell using EM (Hodgson et al., 2014). We have taken advantage of RPA's localization to viral replication centers in MEFs. We analyzed the recruitment of GFP-human RPA32/70 and DDR proteins to nuclear viral replication centers in MEFs. CLEM can provide insight about MuPyV replication centers when immunofluorescence analysis (IFA) of stable cell lines expressing GFP-huRPA32/70 are correlated to EM studies of virus factories.

2. Materials and Methods

Cloning GFP-Tagged RPA32/RPA70 Into a PiggyBac™ Plasmid

Individually GFP-tagged RPA human genes were obtained as plasmids from Marc Wold and cloned into the PiggyBac plasmid (pLP28) containing an ampicillin resistance gene (gift of Amy Palmer). The plasmids (pLP28, GFP-huRPA32, and GFP-huRPA70) were digested with NheI and BamHI. The digests were resolved by electrophoresis and the appropriate bands were excised and purified using the QIAquick gel extraction kit.

The vector (pLP28) and inserts (GFP-huRPA32 or GFP-huRPA70) were ligated. Each ligation was transformed into DH5α *E. coli* and plated on Luria Broth (LB) agar plates containing ampicillin (Amp). Positive clones were screened by restriction digestion with NheI and BamHI. Positive clones (pLP28-huRPA32.1, pLP28-huRPA32.2, pLP28-huRPA70.9, and pLP28-huRPA70.12) were carried forward to generate stable cell lines.

Generation of stable cell lines expressing GFP-tagged RPA proteins

C57 MEFs were maintained in DMEM, supplemented with 10% fetal bovine serum (FBS), penicillin/streptomycin/antimycotic (Sigma A5955) and 55 μM of β-mercaptoethanol (βME) in a humid environment at 37°C and 5% CO_2. For transfection, MEFs were seeded on a six-well dish and allowed to adhere overnight. The following day, each well was transfected with pLP10 (PiggyBac Transposase plasmid) plus one of the following plasmids: pUC18, pLP28, pLP28-huRPA32.1, pLP28-huRPA32.2, pLP28-huRPA70.9, or pLP28-huRPA70.12 using Lipofectamine 2000 in order to generate stable cell lines. (The expression plasmids containing a hygromycin resistance gene were diluted to 100 ng/uL and the pLP10 PiggyBac™ Transposase plasmid was diluted to 40 ng/uL).

The pUC18 plasmid was included in the negative control well in order to bring the total amount of transfected DNA equal to the other wells. The DNA/Lipofectamine mix was added to growth media, and the cells were incubated at 37°C for three days before the media was replaced with fresh growth media containing 50 ug/mL of hygromycin. The cells were incubated and monitored daily for cell death and subsequent growth of hygromycin-resistant cells as stated above.

Inducing DNA damage in stable cell lines expressing GFP-tagged RPA proteins

Stably-transfected C57 cells that expressed either GFP-RPA70 or GFP-RPA32 were grown on imaging dishes (MatTek) The growth media was replaced with Fluorobrite DMEM containing Hoechst dye and imaged on the laser scanning light microscope using the environmental chamber at 37°C, 70% humidity, and 5% CO_2. We outlined a region-of-interest (ROI) with the imaging software (Nikon) and induced DNA damage using the 405 laser at 50% for 1 min within the ROI. The cells were imaged at 30-second intervals for a maximum of 40 min.

Virus Infection

Cells were plated and grown overnight as described above. The next day, the growth media was replaced with starve media (DMEM/0.5% FBS/antibiotics/βME), and incubation was continued for another 16-18 hrs. MuPyV (NG59RA) was prepared for infection by sonication, heat, and centrifugation. Briefly, the virus was sonicated for 1 minute at 75% amplitude and placed at 45°C for 20 min. The cell debris was pelleted by centrifugation at 13,000 rpm for 3 minutes. The virus supernatant was diluted 1:25 with adsorption buffer (Hank's buffer/FBS/10mM Hepes, pH 5.6). The media was aspirated

from the cells and the diluted virus was added to each well and incubated at 37°C. After 1-hour incubation, virus was removed, and normal growth media was added to the wells. The cells were incubated at 37°C for the time indicated for each experiment.

Immunofluorescence Analysis

Cells were plated on acid-etched coverslips and infected as described above. Coverslips were washed twice with cold phosphate buffered saline (PBS) and incubated on ice for 5 minutes in CSK buffer (10 mM PIPES, pH 6.8/100 mM NaCl/300 mM sucrose/3 mM $MgCl_2$/1 mM EGTA/0.5% Triton X-100) with protease inhibitor (Roche, Complete Mini). Coverslips were washed twice with cold PBS and fixed in 4% paraformaldehyde (PFA) for 15 min at room temperature (RT). Following an overnight block in 2% bovine calf serum (BCS) in PBS (blocking buffer) at 4°C, coverslips were incubated with primary antibody at 37°C for 1 hr and washed three times with blocking buffer. The coverslips were incubated with secondary antibody under the same conditions and washed three times with blocking buffer and then mounted using DAPI Prolong Anti-Fade Gold (Invitrogen) and allowed to cure for 24 hrs at RT. Cells were imaged on the Nikon A1R laser-scanning light microscope using 100X objective. Z-stacks through the nucleus were collected; images shown represent a single z-plane through the center of the nucleus. Image J software was used to analyze the images.

Immunofluorescence Antibodies

Primary antibodies used for immunostaining were anti-LT (E1, rat), 1:2000; anti-RPA32 (3A2, rat; gift of H. Nasheuer), 1:5; anti-RPA32-pSer23 (8H3, rat; gift of H. Nahseuer), 1:20; anti-pATM (Millipore, mouse), 1:1000; and anti-γ H2AX (AbCam, rabbit),

1:1000. For RPA32 co-staining with anti-LT antibody, the anti-RPA32 antibody was directly conjugated with AlexaFluor 546 (Invitrogen) and used at a 1:5 dilution after the LT primary and secondary antibody incubations. The secondary antibodies used were conjugated with AlexaFluor 647 (Invitrogen) and used at a 1:2000 dilution. All primary and secondary antibodies were diluted in 2% blocking buffer.

Fluorescent In Situ Hybridization (FISH) of MuPyV DNA

The MuPyV genome (NG59RA) was cloned into pUC18 and a FISH probe was generated by nick translation of pUC18-MuPyV plasmid using Promofluor-550 NT Labeling Kit. Cells were grown on coverslips and infected, fixed, and immunostained for viral and/or host proteins as described above except after secondary antibody staining, the cells were washed three times with PBS, fixed with 4% PFA in PBS, and washed three times with 2% BCS in PBS followed by two washed in 2X SSC. The cells were treated with 0.2 mg/ml RNase Type III (Sigma) in 2X SSC at 37°C for 15 min and washed three times in 2x SSC. The FISH probe was diluted in cDenHyb (InSitus) and hybridized with samples for 3 minutes at 90°C, followed by 2 minutes at each temperature 80°C, 70°C, 60°C, 50°C, 45°C, and finally overnight at 37°C in a humid environment. Coverslips were washed for 5 minutes each at 45°C with 1.5x SSC, 1.5x SSC/50% formamide, and 1.5x SSC and a final wash in PBS. Cells were mounted onto glass slides using DAPI Prolong Anti-Fade Gold (Invitrogen) and allowed to cure for 24 hrs at RT.

High-Pressure Freezing, Freeze Substitution, and Embedding

Stable cell lines expressing GFP-RPA70 or GFP-RPA32 were cultured on T75 flasks and infected with MuPyV (strain NG59RA). The cells were trypsinized and collected by

centrifugation. The cell pellet was resuspended in a small volume cryoprotectant (either 20% dextran/5mM sucrose or 150 mM Mannitol) to make a cell slurry. The slurry was placed into aluminum planchettes (0.1 μm depth) and frozen by high pressure on a Wohlwend Compact 02 high-pressure freezer. After freezing, the hats containing the samples were released immediately into a liquid nitrogen bath and placed in cryotubes containing freeze-substitution media.

Three freeze-substitution (FS) medias in acetone were tested: 0.1% uranyl acetate (UA), 0.025% UA, or acetone alone. Cryotubes containing frozen samples were transferred to a freeze-substitution/low-temperature embedding apparatus (AFS, Leica Microsystems) to allow for user-controlled temperature changes. The samples were warmed to -85°C for 12 hrs. The temperature was then raised to -35°C. The samples were washed with cold acetone, and infiltrated with increasing concentrations of HM20. After three changes in 100% HM20, samples were distributed between four BEEM capsules and the resin was polymerized at -35°C for 24 hrs under UV light and subsequently warmed to RT.

Sectioning, Staining, and Imaging of Embedded Samples

70 nm sections were collected using an (Leica) ultramicrotome equipped with a diamond knife and mounted on nickel and copper grids. The sections were imaged using the Nikon A1R laser-scanning light microscope using 100x objective lens and a 488 laser line, to identify GFP-positive cells. The sections were then post-stained with methanolic 1% UA followed by lead citrate and imaged on the FEI TwinSpirit T12 electron microscope operative at 100kV.

3. Results

Generation of MEFs expressing GFP-tagged human RPA32 or RPA70

The host RPA complex is a ssDNA binding protein that is recruited to sites of vDNA replication. We obtained plasmids containing GFP-tagged human RPA70 or RPA32 from Marc Wold. We cloned the GFP-tagged genes into the PiggyBac Transposase system in order to generate mouse fibroblasts stably expressing human GFP-RPA32 or GFP-RPA70. We digested the pLP28 PiggyBac plasmid and the GFP-huRPA32/70 plasmids with NheI and BamHI. Restriction digests were gel purified using the QIAquick gel extraction kit and the GFP-huRPA genes were ligated into pLP28 using T4 DNA ligase (Fig 3A). The ligations were transformed into DH5α *E. coli* and plated onto Luria-Broth agarose plates containing ampicillin. Colonies were screened with a mini-plasmid prep and digested with NheI and BamHI. Positive clones (pLP28-huRPA32/70) were carried forward to generate stable cell lines (Fig 3B).

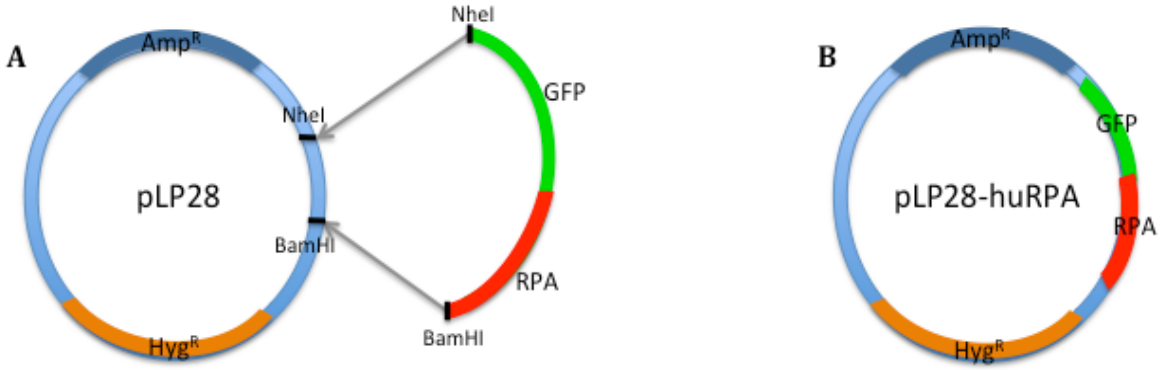

Figure 3. (A) Diagram of the digestion and ligation of pLP28 and GFP-huRPA: black bars indicate sites of digestion with NheI or BamHI; gray arrows indicate sites of insertion of the plasmid encoding GFP-huRPA into the pLP28 plasmid. (B) Diagram of the resulting pLP28-huRPA plasmid after digestion and ligation.

Stable cell lines were generated by transfecting MEFs with either pLP28-GFP-huRPA32 or pLP28-GFP-huRPA70 together with pLP10, the plasmid containing the transposase. Cells that had stable integration of the GFP-huRPA plasmids were selected in growth media containing hygromycin and screened for expression of GFP-RPA32/70.

In order to determine whether the stable cell lines expressed GFP-huRPA32/70, we looked at the cells by light microscopy for GFP expression. Since RPA is recruited to sites of DNA damage and it was tagged with GFP, we expected to see GFP expression when DNA damage was induced. Therefore, we induced DNA damage by irradiating specific sites within the cells and characterizing sites of GFP-huRPA32/70 localization, denoted by an increased intensity of GFP. We found that stable cell lines expressing GFP-huRPA32 (Fig 4) and GFP-huRPA70 (data not shown) displayed an increased intensity of GFP at the site of DNA damage, but not outside of the ROI, by 6 minutes after irradiation. Our results demonstrate that GFP-huRPA32 and GFF-huRPA70 are recruited to sites of induced DNA damage in MEFs.

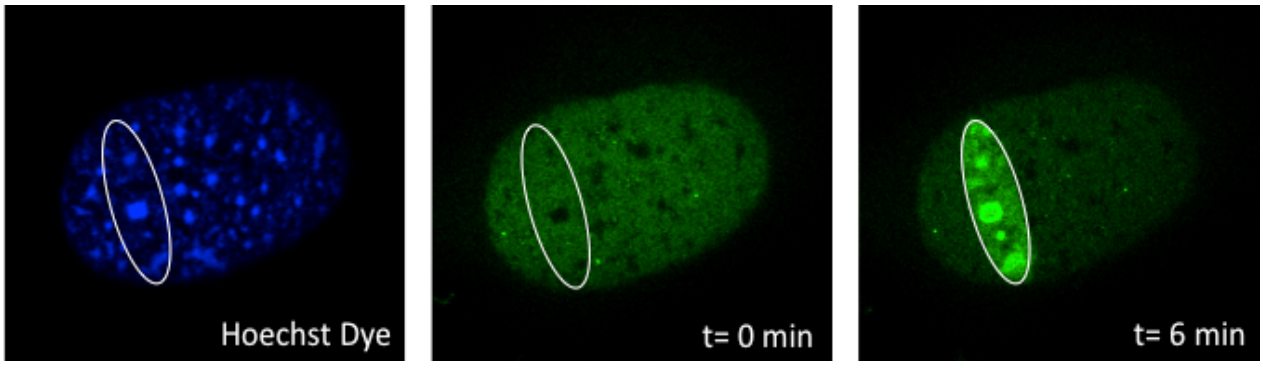

Figure 4. GFP-huRPA32 and GFP-huRPA70 are recruited to sites of DNA damage in stable cell lines. MEFs stably-expressing GFP-huRPA32 were grown on imaging dishes and the nuclei were stained with Hoechst dye. Cells were maintained in an environmental chamber at 37°C, 70% humidity and 5% CO2 during imaging. Region of interests (ROI) were selected using the Nikon software and are denoted by white outlines. DNA damage was induced within the ROI using the 405 laser at 50% for 1 minute. Live cells were imaged before and after irradiation at 1-minute intervals on the Nikon A1R laser-scanning light microscope. Image above shows GFP-huRPA32 before irradiation (t=0 min) and after irradiation (t=6 min).

RPA32 was found previously to co-localize to sites of vDNA replication centers and LT sites during MuPyV infection of MEFs (Heiser et al., 2016). We determined whether stable cell lines expressing GFP-huRPA70 and GFP-huRPA32 could be infected with MuPyV and if so, would GFP-huRPA32/70 localize to sites of vDNA replication and LT. We also determined whether stable cell lines expressing GFP-huRPA70 localized to the same sites as endogenous mouse RPA32 (mu-RPA32). We infected the stable cell line with MuPyV and harvested them at 28 hrs post infection. The cells were then fixed, permeabilized and stained for vDNA, LT, and mu-RPA32. We generated a fish probe by cloning the MuPyV genome into a pUC18 plasmid, followed by nick translation (Erickson, 2012). The FISH probe was hybridized to the samples and the cells were imaged on the Nikon A1R laser-scanning light microscope.

We found that GFP-huRPA70 localized to viral replication centers (Fig 5A) as well as sites of LT (Fig 5A and 5B) and mu-RPA32 (Fig 5B). We also observed GFP-huRPA32's localization to vDNA replication centers, indicating that these cell lines behaved similarly to the GFP-huRPA70 cell lines (data not shown). These results suggest that GFP-huRPA70 is being recruited to the same sites as endogenous mu-RPA32 and may be facilitating vDNA replication by associating with LT.

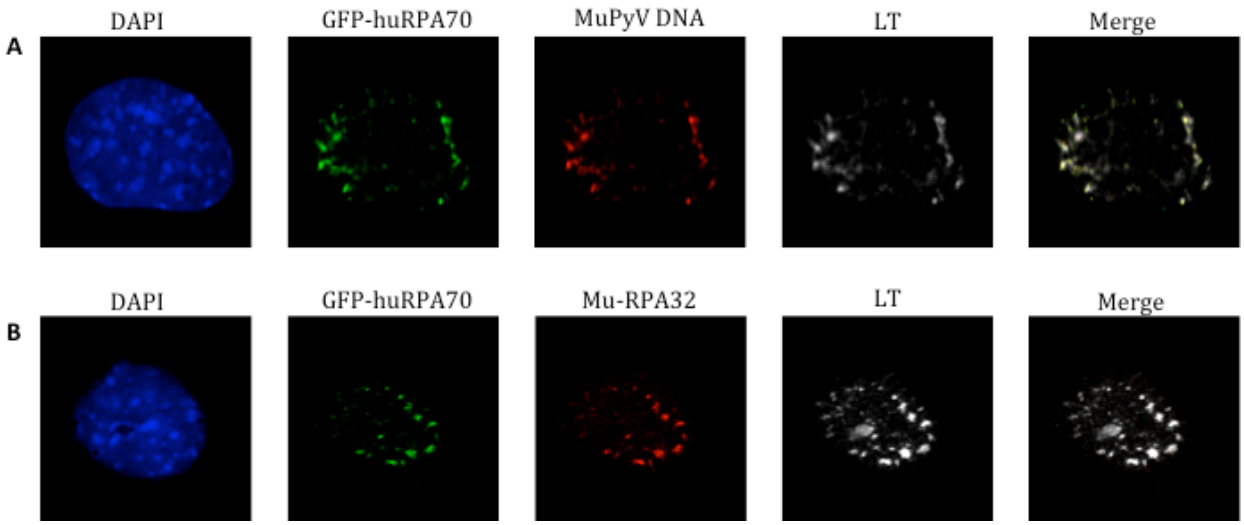

Figure 5. GFP-huRPA32 and GFP-huRPA70 are recruited to sites of vDNA replication. GFP-huRPA70 is also recruited to sites of mu-RPA32 and LT within the nucleus. Stable cell lines expressing GFP-huRPA70 and GFP-huRPA32 were infected with MuPyV (NG59RA), fixed, permeabilized, and immunostained at 28 hours post infection. Images were taken on the A1R light microscope; cells were stained for (**A**) MuPyV DNA (FISH) and LT (**B**) Mu-RPA32 and LT

MuPyV recruits and activates host DDR proteins to sites of vDNA replication (Heiser et al., 2016). We therefore studied the recruitment and activation of host DDR proteins to viral replication centers in stable cell lines expressing GFP-huRPA32/70. We infected the stable cell lines with MuPyV and harvested them at 28 hrs post infection. The cells were then fixed, permeabilized and immunostained for pATM, RPA32-pSer23, and γ H2AX. FISH was performed on the cells to analyze the co-localization of GFP-huRPA32/70 and host DDR proteins with sites of vDNA replication. LM revealed that pATM and RPA32-pSer23 were recruited to sites of GFP-huRPA70 during infection (Fig 6A and 6B). Additionally, the host DDR signaling protein, γ H2AX, localized to sites of GFP-huRPA32 during infection (Fig 6C). The localization of RPA32-pSer23 to sites of GFP-huRPA70 indicates that activated RPA32 was being recruited to these sites. The localization of host DDR proteins to sites of GFP-huRPA32 and GFP-huRPA70 indicate that the human RPA protein may be facilitating

the recruitment of activated endogenous RPA32 (RPA32-pSer23) as well as pATM and γ H2AX.

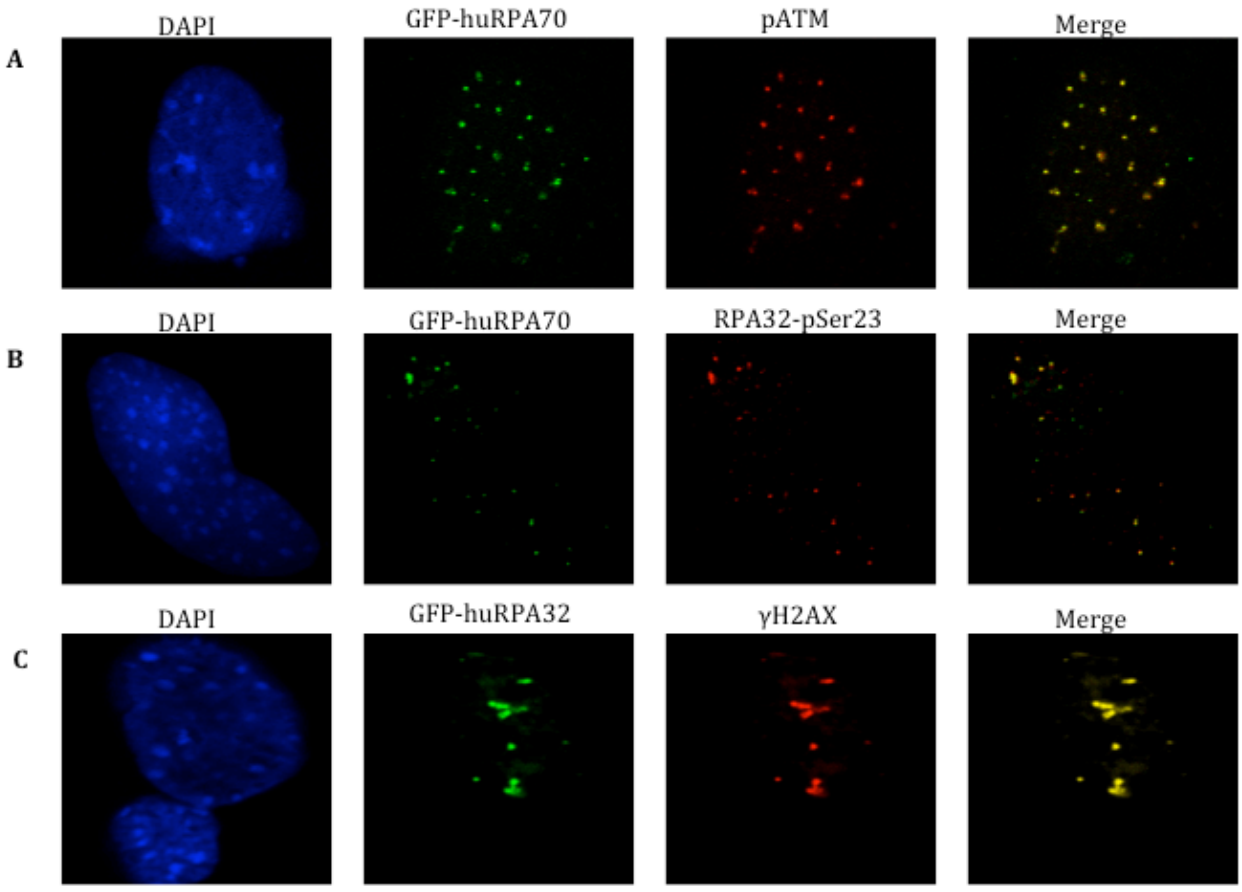

Figure 6. DDR proteins are recruited to sites of vDNA replication in stable cell lines expressing GFP-huRPA32 and GFP-huRPA70. Stable cell lines expressing GFP-huRPA32 or GFP-huRPA70 were infected with MuPyV (NG59RA), fixed, permeabilized, and immunostained at 28 hours post infected. Images were taken on the A1R light microscope; cells were stained for (A) pATM in GFP-huRPA70 cells (B) RPA32-pSer23 in GFP-huRPA70 cells (C) γH2AX in GFP-huRPA32 cells.

CLEM can be used to visualize the subcellular localization of fluorescently-tagged proteins. We analyzed the localization of GFP-huRPA32/70 to sites of vDNA replication and DDR proteins via LM and attempted to study GFP-huRPA32/70's localization to subcellular structures using the high-resolution power of EM. To determine if GFP is retained and virus

factory formation is present in stable cell lines expressing GFP-huRPA32/70 after CLEM processing we infected the stable cell lines with MuPyV and performed high-pressure freezing. The samples were placed in a freeze substitution media and infiltrated with resin that was polymerized under UV light. Sections were generated on the ultramicrotome and imaged on the LM to analyze the retention of fluorescence. Following this, the sections were post-stained and imaged on the EM to analyze virus factory formation. LM of thin sections revealed that GFP fluorescence was not retained after processing. EM of thin sections revealed virions in the nucleus of these cells but since we could not correlate fluorescence with electron micrographs, we were unable to determine if the virions were formed in a cell expressing GFP-huRPA.

4. Discussion

It has been shown previously by LM that endogenous RPA32 localizes to sites of vDNA replication and reorganizes host DDR proteins in the nucleus (Heiser et al., 2016). In addition, it has been shown by EM that MEFs infected with MuPyV demonstrate virus factory formation in the nucleus (Erickson et al., 2012). In order to utilize GFP-huRPA32/70 for CLEM, we analyzed its localization when expressed in MEFs. First, we analyzed GFP-huRPA32/70's recruitment to sites of induced DNA damage within the ROI and found that the human RPAs were appropriately recruited. Following this, we analyzed GFP-huRPA32/70's localization to sites of vDNA replication by infecting the stable cell lines with MuPyV. We found that GFP-huRPA32/70 was recruited to sites of vDNA replication as well as endogenous RPA32 and LT. Our results indicate that stable cell lines expressing GFP-huRPA32/70 can be infected with MuPyV and LT may utilize GFP-huRPA32/70 to facilitate vDNA replication. MuPyV interacts with other host DDR proteins, such as pATM, γH2AX, and RPA32-pSer23, to drive the cell into S phase and promote viral replication. In order to study the recruitment of additional host DDR proteins in stable cell lines expressing GFP-huRPA32/70 we stained the stable cell lines for host DDR proteins and vDNA and imaged them on the LM. Our results indicate that host DDR proteins (pATM, γH2AX, and RPA32-pSer23) were appropriately recruited to sites of GFP-huRPA32/70 during infection. Although it is has been shown that GFP-huRPA proteins are localizing to the appropriate sites, further studies are necessary to determine if the GFP-huRPA proteins are activated. Immunostaining for activated GFP-huRPA32 with a specific antibody against human RPA32-pSer23 may provide this insight. Furthermore, to investigate whether human RPA proteins are sufficient in facilitating vDNA replication independent of

endogenous RPAs, small interfering RNA (siRNAs) may be used to suppress the gene expression of host RPAs. Following endogenous gene suppression, the stable cell lines expressing GFP-huRPA32/70 can be studied for MuPyV infection, localization to viral replication centers, and recruitment of host DDR proteins. These cell lines can also be studied by EM to reveal the characteristics of virus factory formation.

After stable cell lines expressing GFP-huRPA32/70 were high pressure frozen and infiltrated with resin, LM images displayed a lack of fluorescence. In addition, EM images displaying virions were inconclusive due to the inability to correlate virions to fluorescently-tagged RPAs. It has been reported previously that fluorescence is retained after processing using a quick high-pressure freezing protocol (Peddie et al., 2014). Therefore, decreasing the amount of time our samples underwent high-pressure freezing may preserve GFP fluorescence. It has also been shown that CLEM is successful if live cell imaging on the LM is performed prior to processing the cells for EM (Rijnsoever et al., 2008). Therefore, live cell imaging the stable cell lines expressing GFP-huRPA proteins on gridded coverslips may provide points of orientation that can be co-localized to subcellular structures seen by EM. Our results demonstrate that stable cell lines expressing GFP-huRPA32/70 are suitable for optimizing CLEM techniques. Further studies to improve processing and techniques for CLEM will need to be explored.

Acknowledgements

I would like to thank Marc Wold for the plasmids encoding GFP-tagged RPA32 and RPA70 proteins and Amy Palmer for sharing the PiggyBac™ plasmids. I would like to thank the Joe Dragavon and the BioFrontiers Advance Light Microscopy Core Facility for microscopy training and use; Courtney Ozzello, Garry Morgan and the CU-Boulder Electron Microscopy Facility for sample preparation and microscope use. Lastly, I would like to thank Kimberly Erickson for the overwhelming support and time commitment to this project, Dr. Robert Garcea and the Garcea lab for their support and contribution to this thesis.

References

Banerjee, Pubali, Rowena Dejesus, Ole Gjoerup, and Brian S. Schaffhausen. "Viral Interference with DNA Repair by Targeting of the Single-Stranded DNA Binding Protein RPA." *PLoS Pathogens* 9.10 (2013): n. pag. Web. 2 Feb. 2017.

Barouch, Dan H., and Stephen C. Harrison. "Interactions among the Major and Minor Coat Proteins of Polyomavirus." *Journal of Virology* 68.6 (1994): 3982-989. Web. 23 Mar. 2017.

Bassing, C. H., K. F. Chua, J. Sekiguchi, H. Suh, S. R. Whitlow, J. C. Fleming, B. C. Monroe, D. N. Ciccone, C. Yan, K. Vlasakova, D. M. Livingston, D. O. Ferguson, R. Scully, and F. W. Alt. "Increased ionizing radiation sensitivity and genomic instability in the absence of histone H2AX." *Proceedings of the National Academy of Sciences* 99.12 (2002): 8173-178. Web. 3 Mar. 2017.

Bennett, S. M., M. Jiang, and M. J. Imperiale. "Role of Cell-Type-Specific Endoplasmic Reticulum-Associated Degradation in Polyomavirus Trafficking." *Journal of Virology* 87.16 (2013): 8843-852. Web. 24 Mar. 2017.

Borgstahl, Gloria E.o., Kerry Brader, Adam Mosel, Shengqin Liu, Elisabeth Kremmer, Kaitlin A. Goettsch, Carol Kolar, Heinz-Peter Nasheuer, and Greg G. Oakley. "Interplay of DNA damage and cell cycle signaling at the level of human replication protein A." *DNA Repair* 21 (2014): 12-23. Web.

Celeste, Arkady, Oscar Fernandez-Capetillo, Michael J. Kruhlak, Duane R. Pilch, David W. Staudt, Alicia Lee, Robert F. Bonner, William M. Bonner, and André Nussenzweig. "Histone H2AX phosphorylation is dispensable for the initial recognition of DNA breaks." *Nature Cell Biology* 5.7 (2003): 675-79. Web. 3 Mar. 2017.

Chen, X. S. "Interaction of polyomavirus internal protein VP2 with the major capsid protein VP1 and implications for participation of VP2 in viral entry." *The EMBO Journal* 17.12 (1998): 3233-240. Web. 31 Mar. 2017.

Cheng, Jingwei, James A. Decaprio, Michele M. Fluck, and Brian S. Schaffhausen. "Cellular transformation by Simian Virus 40 and Murine Polyoma Virus T antigens." *Seminars in Cancer Biology* 19.4 (2009): 218-28. Web. 10 Mar. 2017.

Ciccia, Alberto, and Stephen J. Elledge. "The DNA Damage Response: Making It Safe to Play with Knives." *Molecular Cell* 40.2 (2010): 179-204. Web. 23 Mar. 2017.

D'amours, Damien, and Stephen P. Jackson. "The mre11 complex: at the crossroads of dna repair and checkpoint signalling." *Nature Reviews Molecular Cell Biology* 3.5 (2002): 317-27. Web. 24 Mar. 2017.

Decaprio, James A., and Robert L. Garcea. "A cornucopia of human polyomaviruses." *Nature Reviews Microbiology*11.4 (2013): 264-76. Web. 12 Dec. 2016.

Erickson, Kimberly D., Cedric Bouchet-Marquis, Katie Heiser, Eva Szomolanyi-Tsuda, Rabinarayan Mishra, Benjamin Lamothe, Andreas Hoenger, and Robert L. Garcea. "Virion Assembly Factories in the Nucleus of Polyomavirus-Infected Cells." *PLoS Pathogens* 8.4 (2012): n. pag. Web. 15 Mar. 2017.

Fanning, E. "A dynamic model for replication protein A (RPA) function in DNA processing pathways." *Nucleic Acids Research* 34.15 (2006): 4126-137. Web. 2 Dec. 2016.

Fanning, Ellen , Xiaorong Zhao, and Xiaohua Jiang. "Polyomavirus Life Cycle." *DNA Tumor Viruses*. New York: Springer Science and Business Media, 2009. 23-38. Print.

Fotedar, R., and JM Roberts. "Cell-Cycle Regulated Phosphorylation of RPA-32 Occurs Within the Replication Initiation Complex." *EMBO Journal* 11.6 (n.d.): 2177-187. Web. 5 Mar. 2017.

Gardner, Sylviad., Annem. Field, Dulciev. Coleman, and B. Hulme. "New Human Papovavirus (B.k.) Isolated From Urine After Renal Transplantation." *The Lancet* 297.7712 (1971): 1253-257. Web. 26 Feb. 2017.

Gilbert, J. M., I. G. Goldberg, and T. L. Benjamin. "Cell Penetration and Trafficking of Polyomavirus." *Journal of Virology* 77.4 (2003): 2615-622. Web. 3 Mar. 2017.

Goodwin, E. C., A. Lipovsky, T. Inoue, T. G. Magaldi, A. P. B. Edwards, K. E. Y. Van Goor, A. W. Paton, J. C. Paton, W. J. Atwood, B. Tsai, and D. Dimaio. "BiP and Multiple DNAJ Molecular Chaperones in the Endoplasmic Reticulum Are Required for Efficient Simian Virus 40 Infection." *MBio* 2.3 (2011): n. pag. Web. 24 Mar. 2017.

Guy, C. T., R. D. Cardiff, and W. J. Muller. "Induction of mammary tumors by expression of polyomavirus middle T oncogene: a transgenic mouse model for metastatic disease." *Molecular and Cellular Biology* 12.3 (1992): 954-61. Web. 10 Mar. 2017.

Han, Yufeng, Yueh-Ming Loo, Kevin T. Militello, and Thomas Melendy. "Interactions of the Papovavirus DNA Replication Initiator Proteins, Bovine Papillomavirus Type 1 E1 and Simian Virus 40 Large T Antigen, with Human Replication Protein A." *Journal of Virology* 73.6 (1999): 4899-907. Web. 2 Dec. 2016.

Heiser, Katie, Catherine Nicholas, and Robert L. Garcea. "Activation of DNA damage repair pathways by murine polyomavirus." *Virology*497 (2016): 346-56. *Pubmed*. Web. 12 Dec. 2016.

Henricksen, L. "Phosphorylation of human replication protein A by the DNA-dependent protein kinase is involved in the modulation of DNA replication." *Nucleic Acids Research* 24.15 (1996): 3107-112. Web. 5 Mar. 2017

Hirsch, Hans H., and Jürg Steiger. "Polyomavirus BK." *The Lancet Infectious Diseases* 3.10 (2003): 611-23. Web. 10 Mar. 2017.

Hodgson, Lorna, David Nam, Judith Mantell, Alin Achim, and Paul Verkade. "Retracing in Correlative Light Electron Microscopy: Where is My Object of Interest?" *Correlative Light and Electron Microscopy II*. Vol. 124. N.p.: Elsevier Inc., 2014. 1-21. Print.

Justice, Joshua L., Brandy Verhalen, and Mengxi Jiang. "Polyomavirus interaction with the DNA damage response." *Virologica Sinica* 30.2 (2015): 122-29. Web. 5 Mar. 2017.

Kawano, M.-A., T. Inoue, H. Tsukamoto, T. Takaya, T. Enomoto, R.-U Takahashi, N. Yokoyama, N. Yamamoto, A. Nakanishi, T. Imai, T. Wada, K. Kataoka, and H. Handa. "The VP2/VP3 Minor Capsid Protein of Simian Virus 40 Promotes the in Vitro Assembly of the Major Capsid Protein VP1 into Particles." *Journal of Biological Chemistry* 281.15 (2006): 10164-0173. Web. 4 Mar. 2017.

Kenny, Mark K , Uwe Schlege, Henry Furneaux, and Jerard Hurwitz. *The Journal of Biological Chemistry* 265.13 (1990): 7693-000. Web. 5 Mar. 2017.

Klein, G. "Organization and Expression of the Genome of Polyoma Virus." *Viral Oncology* (1980): 447-80. Web. 26 Feb. 2017.

Liu, Qinghua, Saritha Guntuku, Xian-Shu Cui, Shuhei Matsuoka, David Cortez, Katsuyuki Tamai, Guangbin Luo, Sandra Carattini-Rivera, Francisco DeMayo, Allan Bradley, Larry Donehower, and Stephen Elledge. "Chk1 is an essential kinase that is regulated by Atr and required for the G2/M DNA damage checkpoint." *Genes & Development* 14.12 (2000): 1448-459. Web. 23 Mar. 2017.

Maginnis, Melissa S., Christian D. S. Nelson, and Walter J. Atwood. "JC polyomavirus attachment, entry, and trafficking: unlocking the keys to a fatal infection." *Journal of NeuroVirology* 21.6 (2014): 601-13. Web. 10 Mar. 2017.

Matsuoka, S., B. A. Ballif, A. Smogorzewska, E. R. Mcdonald, K. E. Hurov, J. Luo, C. E. Bakalarski, Z. Zhao, N. Solimini, Y. Lerenthal, Y. Shiloh, S. P. Gygi, and S. J. Elledge. "ATM and ATR Substrate Analysis Reveals Extensive Protein Networks Responsive to DNA Damage." *Science* 316.5828 (2007): 1160-166. Web. 2 Mar. 2017.

Myers, Richard M., Donald C. Rio, Alan K. Robbins, and Robert Tjian. "SV40 gene expression is modulated by the cooperative binding of T antigen to DNA." *Cell* 25.2 (1981): 373-84. Web. 23 Mar. 2017.

Nakanishi, A., N. Itoh, P. P. Li, H. Handa, R. C. Liddington, and H. Kasamatsu. "Minor Capsid Proteins of Simian Virus 40 Are Dispensable for Nucleocapsid Assembly and Cell Entry but Are Required for Nuclear Entry of the Viral Genome." *Journal of Virology* 81.8 (2007): 3778-785. Web. 3 Mar. 2017.

Neu, Ursula, Thilo Stehle, and Walter J. Atwood. "The Polyomaviridae: Contributions of virus structure to our understanding of virus receptors and infectious entry." *Virology* 384.2 (2009): 389-99. Web. 3 Mar. 2017.

Norkin, L. C., H. A. Anderson, S. A. Wolfrom, and A. Oppenheim. "Caveolar Endocytosis of Simian Virus 40 Is Followed by Brefeldin A-Sensitive Transport to the Endoplasmic Reticulum, Where the Virus Disassembles." *Journal of Virology* 76.10 (2002): 5156-166. Web. 3 Mar. 2017.

O'Hara, Samantha D., and Robert L. Garcea. "Murine Polyomavirus Cell Surface Receptors Activate Distinct Signaling Pathways Required for Infection." *MBio* 7.6 (2016): n. pag. *Pubmed*. Web. 12 Dec. 2016.

Peddie, Christopher J., Ken Blight, Emma Wilson, Charlotte Melia, Jo Marrison, Raffaella Carzaniga, Marie-Charlotte Domart, Peter O'toole, Banafshe Larijani, and Lucy M. Collinson. "Correlative and integrated light and electron microscopy of in-resin GFP fluorescence, used to localise diacylglycerol in mammalian cells." *Ultramicroscopy* 143 (2014): 3-14. Web. 30 Mar. 2017.

Perkovic, Mario, Michael Kunz, Ulrike Endesfelder, and Stefanie Bunse. "Correlative Light- and Electron Microscopy with chemical tags." *Journal of Structural Biology* 186.2 (2014): 205-13. *ScienceDirect*. Web. 4 Dec. 2016.

Rijnsoever, Carolien Van, Viola Oorschot, and Judith Klumperman. "Correlative light-electron microscopy (CLEM) combining live-cell imaging and immunolabeling of ultrathin cryosections." *Nature Methods* 5.11 (2008): 973-80. Web. 24 Mar. 2017.

Rinaldo, Christine Hanssen, Garth D. Tylden, and Biswa Nath Sharma. "The human polyomavirus BK (BKPyV): virological background and clinical implications." *Apmis* 121.8 (2013): 728-45. Web. 10 Mar. 2017.

Tsai, B. "Gangliosides are receptors for murine polyoma virus and SV40." *The EMBO Journal* 22.17 (2003): 4346-355. Web. 3 Mar. 2017.

Yan, Youwei, Thilo Stehle, Robert C. Liddington, Haiching Zhao, and Stephen C. Harrison. "Structure determination of simian virus 40 and murine polyomavirus by a combination of 30-fold and 5-fold electron-density averaging." *Structure* 4.2 (1996): 157-64. Web. 26 Feb. 2017.

Zhao, X., R. J. Madden-Fuentes, B. X. Lou, J. M. Pipas, J. Gerhardt, C. J. Rigell, and E. Fanning. "Ataxia Telangiectasia-Mutated Damage-Signaling Kinase- and Proteasome-

Dependent Destruction of Mre11-Rad50-Nbs1 Subunits in Simian Virus 40-Infected Primate Cells." *Journal of Virology* 82.11 (2008): 5316-328. Web. 24 Mar. 2017.